In vivo study of photosensitizer pharmacokinetics by fluorescence transillumination imaging

Marina Shirmanova
Elena Zagaynova
Marina Sirotkina
Ludmila Snopova
Nizhny Novgorod State Medical Academy
10/1 Minin and Pozharsky sq.
603005 Nizhny Novgorod, Russia

Irina Balalaeva
Irina Krutova
Nataliya Lekanova
N.I. Lobachevsky State University of Nizhny Novgorod
23 Gagarin Avenue
603950 Nizhny Novgorod, Russia

Ilya Turchin
Anna Orlova
Michail Kleshnin
Russian Academy of Sciences
Institute of Applied Physics
46 Ulyanov Street
603950 Nizhny Novgorod, Russia

Abstract. The possibility of *in vivo* investigation of the pharmacokinetics of photosensitizers by means of fluorescence transillumination imaging is demonstrated. An animal is scanned in the transilluminative configuration by a single source and detector pair. Transillumination is chosen as an alternative approach to reflection imaging. In comparison with the traditional back-reflection technique, transillumination is preferable for photosensitizer detection due to its higher sensitivity to deep-seated fluorophores. The experiments are performed on transplantable mouse cervical carcinomas using three drugs: photosens, alasens, and fotoditazin. For quantitative evaluation of the photosensitizer concentration in tumor tissue the fluorescence signal is calibrated using tissue phantoms. We show that the kinetics of photosensitizer tumor uptake obtained by transillumination imaging *in vivo* agree with data of standard *ex vivo* methods. The described approach enables rapid and cost-effective study of newly developed photosensitizers in small animals. [DOI: 10.1117/1.3478310]

Keywords: photosensitizer; pharmacokinetics; mouse cervical carcinoma; fluorescence transillumination imaging; *in vivo*.

Paper 10060R received Feb. 5, 2010; revised manuscript received Jun. 17, 2010; accepted for publication Jun. 24, 2010; published online Aug. 25, 2010.

1 Introduction

Photodynamic therapy (PDT) is an emerging modality for cancer treatment based on light activation of photosensitive dyes called photosensitizers. In the presence of tissue oxygen, this activation results in generation of free radicals and singlet oxygen that destroy neoplastic tissue.[1–3] In addition to photodynamic action, most photosensitizers also produce fluorescence, which enables diagnosis of lesions and pharmacokinetics studies. Currently, PDT is a clinically approved technique for the destruction of small and superficial tumors of different localizations, such as skin cancer, bladder cancer, bronchial cancers, vulvar and early cervical cancers, early lung cancer, Barrett's esophagus, and cancers of the biliary tract.[2–5] PDT may be used interstitially in the cases of tumors of the prostate and brain and residual disease in intraperitoneal carcinomatosis.[6–8] The efficiency of PDT depends on the photosensitizer concentration, the tumor-to-normal-tissue ratio, and the interval between photosensitizer administration and irradiation.[9] As the photosensitizer accumulation, excretion, and distribution kinetics in normal tissues determines its phototoxic properties, it is important to study them in terms of minimization of photodynamic action on skin and mucosa.

Recently, numerous photosensitizers have been developed. Among them are phthalocyanines, naphthalocyanines, porphyrins, benzoporphyrins, chlorins, bacteriochlorin, purpurine, texaphyrins, and porphycenes.[10,11] The recent strategy is directed toward selective delivery of photosensitizer to the tumor tissue, e.g., by conjugation to biomolecules such as monoclonal antibodies.[12–14] For fluorescent diagnostics and PDT, photosensitizers with absorption in the red wavelength range (650 to 850 nm) are preferable because in this spectral region the maximum penetration depth of light into a tissue can be obtained.

In preclinical studies, transplantable mouse tumors are most commonly used for drug evaluation. Unlike human tumor xenografts, which are generally grown in hamster cheek pouches or in athymic nude mice, they are mouse-derived tumors in mice. Advantages of these models over human tumor xenografts include their low cost, reproducibility, and growth in an immune-competent host.[15] A number of transplantable tumors of various histotypes and different growth rates within each histotype were used in preclinical studies of photosensitizers.[16]

Currently, *ex vivo* methods are commonly used in preclinical study of new photosensitive dyes. Drug levels in tissue are quantified by tissue extraction or radiolabeling methods.[17–22] These techniques give accurate data on photosensitizer concentration in tissue samples but they are labor and time consuming and require many animals for each study. To investigate tumor selectivity of photosensitizer and its distribution in tissues, fluorescence confocal microscopy, fluorescence or absorption spectroscopy *in situ*, and high-resolution fluorescence microendoscopy have been employed.[23–26] These methods are based on point measurements. As tumors are spatially and temporally heterogeneous, essential data spread is observed and multiple measurements are required to decrease

Address all correspondence to: Marina Shirmanova, Nizhny Novgorod State Medical Academy, 10/1 Minin and Pozharsky sq., Nizhny Novgorod, 603005, Russia. Tel: 78314654113. Fax: 78314655904. E-mail: shirmanovam@mail.ru

1083-3668/2010/15(4)/048004/8/$25.00 © 2010 SPIE

error. Moreover, they enable examination of only the tissue surface and lack the capability to detect deep-seated fluorophores.

Noninvasive real-time visualization of fluorophores in small animals can be achieved by whole-body fluorescence imaging.[27–30] A number of fluorophores, such as cyanine dyes, quantum dots, fluorescent proteins, and photosensitizers have been imaged in small animals *in vivo*.[31–35] Among the fluorescence imaging techniques, fluorescence diffuse tomography (FDT) is definitely a more advanced technique, enabling 3-D volumetric imaging[27] of fluorescent agents in deep tissues with a resolution of 1 to 2 mm. Nontomographic imaging, both planar reflectance and transillumination modality, is considered to be an alternative approach for fluorescence detection in living organisms.[36–40] Planar reflectance imaging (or epi-illumination) is the most widely exploited but its application is restricted to observation of superficial lesions.[30,35] The transillumination method enables deep-tissue imaging,[38,40] which is especially important for photosensitizer distribution study. Being technically easy to implement and simple in operation in comparison with FDT, it is an attractive tool for pharmacokinetics research.

This work is focused on *in vivo* investigation of photosensitizer pharmacokinetics in mice bearing transplantable tumors. Our goal was the application of transillumination fluorescence imaging to pharmacokinetics study. We assessed fluorescence in a tumor area by 2-D images acquired by synchronous scanning of the object with a single source and detector pair in a transilluminative configuration. The device was initially developed for fluorescence diffuse tomography of tumors labeled with fluorescent proteins in small animals.[41] However, to obtain 3-D information about fluorophore distribution many source-detector measurements are necessary. For a setup with a single source and detector pair, the data acquisition time is too great for photosensitizer pharmacokinetic investigation. This time can be essentially decreased if one uses many detectors or a high-sensitivity CCD. An example of 3-D reconstruction of the photosensitizer in tissue phantoms using subsurface FDT is shown in Ref. 42.

For *in vivo* imaging, a nonpigmented solid epithelial tumor is prefered. We selected mouse cervical carcinoma for the pharmacokinetics investigation because of its slow growth rate, lack of large necrosis, and spherical nodes. The level of photosensitizer accumulation in tumor is known to depend on the dose of the administered specimen. Therefore, to verify whether the signal level in the tumor correctly represents the photosensitizer content we studied the dose-dependent kinetics of accumulation and clearance. The dynamics of accumulation in tumor of three clinically approved photosensitizers with known pharmacokinetics was investigated *in vivo*. For quantitative evaluation of the photosensitizer concentration in tumor tissue, the fluorescence signal was calibrated using tissue phantoms, and the absolute specimen concentration in tumor was determined.

2 Materials and Methods

2.1 *Mice and Tumors*

Experiments were performed on 35 female CBA mice bearing cervical carcinomas. Mouse cervical carcinoma forms mainly spherical nodes and is characterized by a slow growth rate. Microscopically, the tumor is rich in cell components and contains irregularly defined negligible necrotic areas. Hence, by virtue of its morphological and growth features, mouse cervical carcinoma is suitable for *in vivo* fluorescence imaging of photosensitizers using a transillumination imaging setup. Tumors were grown in the subscapular region. Transplantation was made by subcutaneous injection of tumor tissue suspension in nutrient medium. Tumors of the same uniform 8- to 10-mm diameter (14 to 20 days after transplantation) were employed. The tumor was transplanted subcutaneously and during scanning was located on one side of the body so that its projection showed no tissues except the skin covering the tumor.

2.2 *Photosensitizers*

Three drugs were used in the study—photosens, alasens, and fotoditazin—because their tumor selectivity and pharmacokinetics properties have already been completely described.[24,43–45]

Photosens is sulfo-substituted aluminium phthalocyanine[43] (Niopic, Russia). The mice were injected with photosens (1 mg/kg) via the intra verious (i.v.) delivery route (in the lateral tail vein). In aqueous solution, photosens shows maximum absorption at 675 nm and fluorescence at 685 nm.

Alasens (Niopic, Russia) is a preparation[44] on the basis of 5-aminolaevulinic acid (ALA). Although ALA is itself nonfluorescent, it induces[7,17,20,23] accumulation in tumor of endogenous protoporphyrin IX (Pp IX). Pp IX exhibits fluorescence with maxima at 635 and 700 nm. Alasens was administered per os in a dose of 400 mg/kg.

Fotoditazin is N-methyl glucosamine chlorin e6 salt[45] (Veta-Grand, Russia). It has a powerful absorption band with maximum at 662 nm. The fluorescence maximum lies around 675 nm. The mice were injected with 5, 10, or 25 mg/kg fotoditazin i.v. All the administered doses of the photosensitizers did not exceed the therapeutic ones converted from humans to mice.

2.3 *In Vivo Fluorescence Imaging*

We performed the imaging with a setup developed at the Institute of Applied Physics of the Russian Academy of Sciences (Nizhny Novgorod). In this setup, synchronous scanning of the object in transilluminative configuration is provided by a single source-detector pair (Fig. 1). The investigated object is placed between source and detector. For each position of the source-detector pair, a fluorophore located within the sensitivity area makes a contribution to the fluorescence signal. Thus, the detected signal is summed from the fluorescence intensities that come from different depths. Thus, the obtained images (see, e.g., Fig. 3 in Sec. 3) enable assessing a 2-D distribution of the photosensitizer integrated over depth (sensitivity area). A semiconductor laser at 635 nm was chosen as a source of exciting light. A high-sensitivity cooled photomultiplier tube (Hamamatsu H7422-20) was used as a detector of fluorescence light. The emission signal was filtered using a 685- to 735-nm bandpass filter. For the scanning procedure, a depilated animal was fixed vertically in a glass container and slightly compressed to 1.2 cm. The image acquisition time was 3 to 5 min per animal. To investigate the photosensitizer pharmacokinetics, the mice were imaged *in*

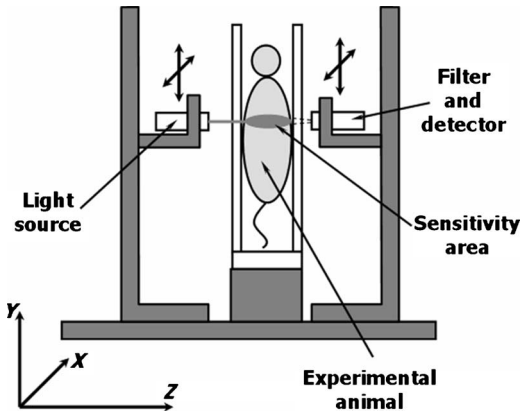

Fig. 1 Schematic of the fluorescence imaging setup. Synchronous scanning of the experimental animal in transilluminative configuration is provided by a single source-detector pair.

vivo for 15 min and 1, 2, 3, 4, 6, and 24 h following the chemicals administration. The image obtained before injection was used as a control.

The fluorescence images were analyzed using ImageJ software (U.S. National Institutes of Health). During data processing we averaged the signal intensity over the tumor area. Mean ± standard deviation (SD) values were used for data representation.

For quantitative assessment of photosensitizer in tumors, the fluorescence signal intensity was calibrated using a model medium of lipofundin and Indian ink. The absorption and reduced scattering coefficients of the medium were chosen close to the average parameters of the tumor for the excitation and emission wavelengths. Calibration curves (Fig. 2), which represent the dependence of the fluorescence signal on the fluorophore concentration, were obtained for fotoditazin, photosens, and Pp IX disodium salt (Sigma-Aldrich). We estimated signal values in a medium with a fotoditazin concentration up to 8 μg/ml, a photosens concentration up to 0.8 μg/ml, and a Pp IX concentration up to 9 μg/ml.

It is clear from the plot that, at small photosensitizer concentrations in the model medium, the fluorescence signal linearly depends on the concentration. At larger concentrations, the signal intensity deviates from the linear dependence as a result of high absorption of the excition light by the photosensitizer.

2.4 *Ex Vivo Fluorescence Measurements*

On imaging 6 and 24 h after injection, the animals were euthanized, and the tumors and normal organs and tissues were removed. The accumulation of the photosensitizer in the tumors was confirmed using the inverted laser scanning confocal fluorescence microscope (Axiovert 200M LSM 510 META, Carl Zeiss, Germany). For microscopic imaging we used excitation at 633 nm and signal collection in the 650- to 710-nm range. Fluorescence was also measured *ex vivo* using a spectrometer (QE65000, Ocean Optics Inc., United States). Tissue samples were excited with 635-nm light, and the emission was collected between 660 and 760 nm. Spearman's rank correlation between the signal value in tumor area from transillumination images *in vivo* and

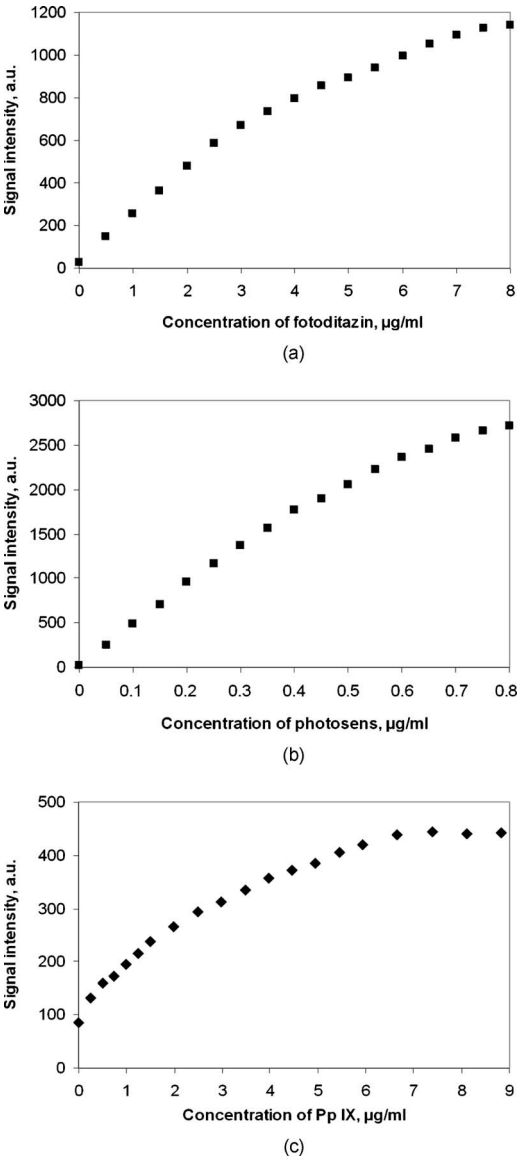

Fig. 2 Calibration of the fluorescence signal in a model medium of lipofundin and Indian ink. Fluorescence signal versus photosensitizer concentration for (a) fotoditazin, (b) photosens, and (c) Pp IX.

integral fluorescence intensity in spectra *ex vivo* was estimated.

A standard morphological examination of tumors was carried out. After fluorescence imaging tumors were resected, fixed with a 10% formalin solution, and prepared in paraffin-embedded tissue blocks. We stained 5-μm sections with hematoxylin and eosin and examined microscopically with 40 × magnification.

3 Results and Discussions

3.1 *In Vivo Fluorescence Imaging of Tumor with Photosensitizer*

Figure 3 demonstrates an example of serial imaging of the CBA mouse bearing a subcutaneous cervical carcinoma. *In vivo* images of the animal injected i.v. with fotoditazin dose of 10 mg/kg are presented. One can see in the figure that the

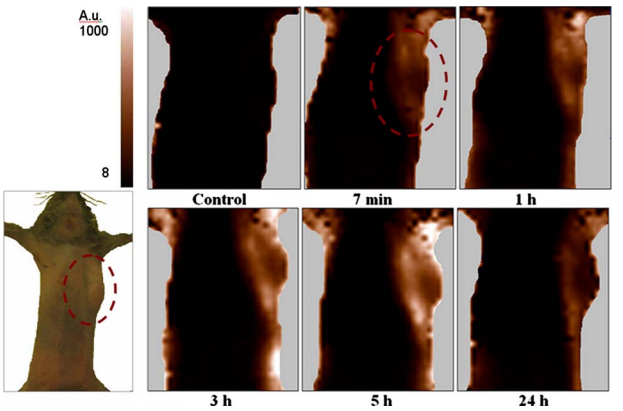

Fig. 3 *In vivo* fluorescence images of a tumor-bearing mouse before (control) and after administration of fotoditazin (10 mg/kg, i.v). Subcutaneously transplanted cervical carcinoma in the right image. Tumor volume is 250 mm^3. Images obtained in transillumination configuration of source and detector of fluorescence imaging setup. Image size is 30×40 mm. Tumor is shown by a dashed curve.

control image acquired before administration of the specimen has low signal intensity and is dark-colored. After administration, an increase of signal intensity in the cervical carcinoma is observed, indicating selective accumulation of the photosensitizer. As a result, tumor fluorescence is brighter than in the adjacent peritumoral tissues. Then, the signal intensity in the tumor area reduces as the specimen is washed out.

After injection of fotoditazin and photosens, tumors could be clearly distinguished from the surrounding tissue in the 15-min to 6-h postinjection period. Maximum signal intensity occurred 1 and 3 h after injection, correspondingly. After oral administration of alasens, we detected a smooth signal growth in tumor area. The signal level was gradually increasing up to 6 h.

Typically, a high signal level is visualized in images of tense skin sections due to their high transparency of light. As mouse skin thickness is small in comparison with tumor diameter, and the photosensitizer accumulation in tumor tissue is 2 to 14 times more than in skin,[17–19,21,46–48] we can speak about a weak contribution of normal tissues to the fluorescence signal in the tumor image.

3.2 *Study of Photosensitizer Fluorescence by Means of Standard Ex Vivo Methods*

For verification of photosensitizer accumulation in tumor tissue, fluorescence was analyzed by standard methods—fluorescence confocal microscopy and fluorescence spectroscopy *ex vivo*.

Figure 4 demonstrates that no significant fluorescence was detected in tumors of mice without photosensitizer; whereas 6 h after agent administration, intense fluorescence was visualized in microscopic images of neoplastic tissue and in the spectra.

The spectra of cancer tissue sensitized with photosens, fotoditazin, and 5-ALA-induced Pp IX were nearly identical in shape to those of photosensitizer solution. A comparison of the fluorescence data from the transilluminative imaging with the accompanying spectroscopic measurements showed a strong correlation. The point is that when the signal is integrated over depth and then averaged over the entire area of the tumor in the transillumination image, its magnitude correlates well with the fluorescence measured spectroscopically. The correlation analysis revealed a correlation coefficient of 0.76 ($P < 0.05$) for photosens, 0.9 ($P < 0.001$) for fotoditazin, and 0.85 ($P < 0.02$) for 5-ALA-induced Pp IX. This means that the influence of various factors, apart from the fluorescence of the photosensitizer localized in tumor tissue, on average signal intensity in tumor area is insignificant. We can refer to these factors as nonuniform photosensitizer distribution in tumor, its histological heretogeneity, and fluorescence of the skin covering the tumor. Thus, the proposed method is sufficiently accurate for assessing photosensitizer fluorescence all over the tumor.

3.3 *Dose-Dependent Pharmacokinetics of Photosensitizer*

Results of *in vivo* signal measurements in the tumor area were used to investigate fotoditazin pharmacokinetics as a function of the administered specimen dose. Pharmacokinetic curves are plotted for three therapeutic doses of fotoditazin administered *in vivo*: 5, 10, and 25 mg/kg (Fig. 5). As was to be expected, tumors of the animals with a small dose had a low fluorescence signal, whereas tumors of the animals with the larger dose had a higher fluorescence intensity. The shapes of the curves suggest a small difference between the kinetics of photosensitizer uptake. For a dose of 5 mg/kg, the signal intensity reached its maximum 1 h after injection, and reduced gradually afterward. For a dose of 10 mg/kg, the maximum accumulation was observed in the period from 3 to 6 h after injection. When a dose of 25 mg/kg was administered, we detected the strongest signal in the tumor 2 to 7 h after injection. In 24 h, the fluorescence in the tumor was still detectable for all of the doses, but its intensity was substantially lower because of photosensitizer clearance from the organism.

Several authors have shown that fotoditazin and chlorin e6 derivative compounds exhibit rapid tumor uptake and clearance from the organism.[18,49] Maximum tumor uptake of fotoditazin was reported to be 1 h after injection with the maximum tumor-to-normal-tissue ratio 4 to 6 h after injection; 94% of the drug initial dose was washed out 24 h after injection.[49] Thus, our results on fotoditazin accumulation and clearance kinetics are similar to the data in the literature obtained by complicated tissue extraction methods.

We found that at the photosensitizer accumulation maximum, the dependence of signal level in tumor on administered dose is close to linear an with approximately 0.95 reliability. Our data on the linear dependence of tumor fluorescence on drug dose agree with those available in the literature. A linear increase of chlorin-based photosensitizer concentrations in tissue was observed[18] with doses of the administered drug increasing up to 50 mg/kg. Based on those findings and the results of fluorescence imaging we can state that signal intensity in tumor quantitatively represents fluorophore content.

3.4 *Kinetics of Accumulation of Different Photosensitizers in Tumor In Vivo*

The results of fluorescence imaging *in vivo* showed that different photosensitizers have different kinetics of tumor uptake. We assessed concentrations of photosensitizers in tumor

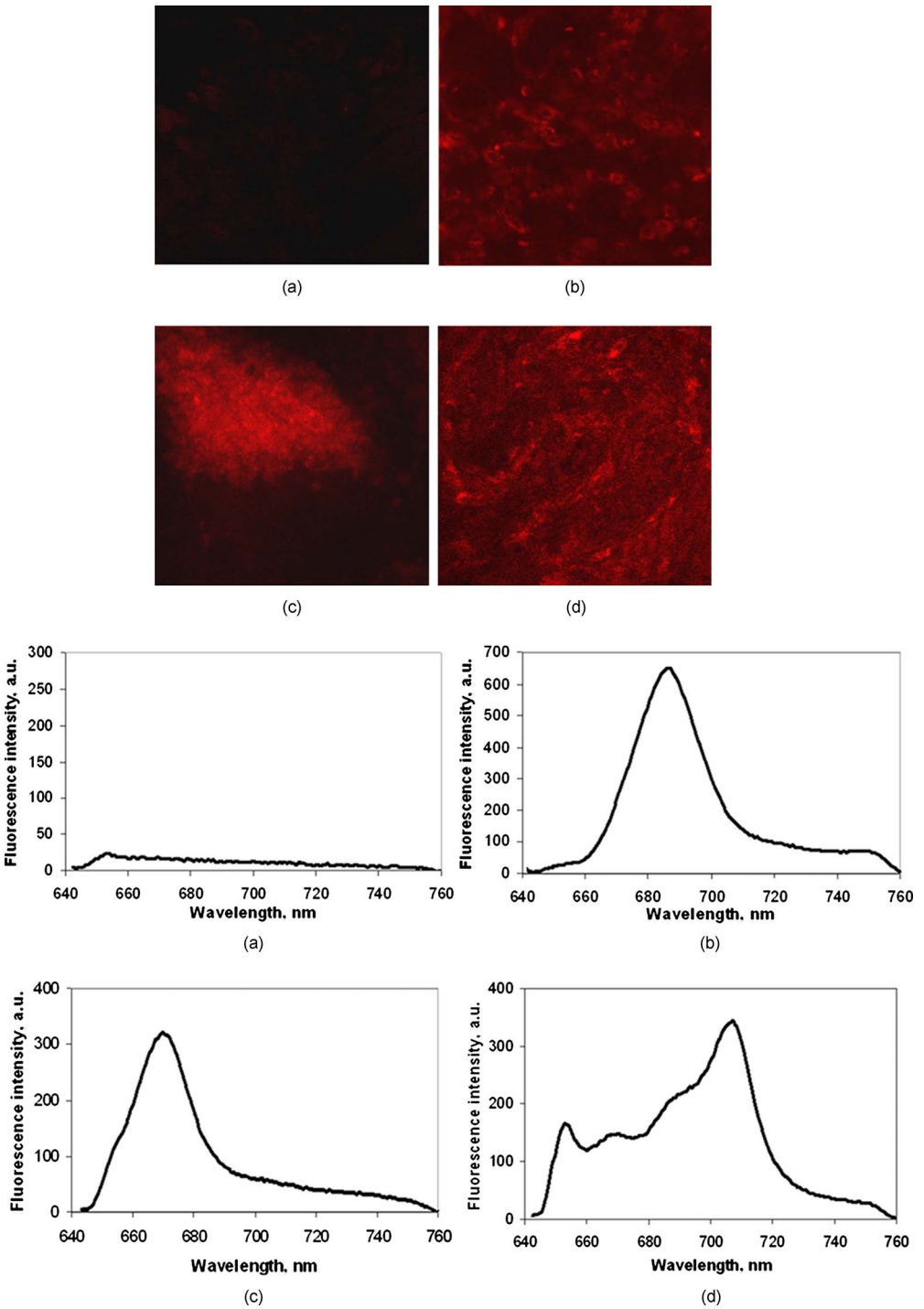

Fig. 4 Representative confocal fluorescence images and fluorescence spectra of the mouse cervical carcinoma *ex vivo*: (a) no photosensitizer, (b) photosens, (c) fotoditazin, and (d) 5-ALA-induced Pp IX; 6 h after administration.

in vivo by means of calibration curves. The obtained plots of specimen accumulation in tumor tissue are demonstrated in Fig. 6. At the accumulation maximum, the photosens concentration in tissue was about 0.27 μg/g for an administered dose of 1 mg/kg, the fotoditazin concentration was about 4 μg/g for a dose of 25 mg/kg, and the 5-ALA-induced Pp IX concentration was about 6 μg/g for an alasense dose of 400 mg/kg.

The features of the dynamics of photosensitizer accumulation in experimental tumors of mice *in vivo* revealed by our team are in a good agreement with earlier results obtained by other researchers using standard methods.[17,20,21,24,25,46,49]

To explain of the difference in the obtained kinetic curves it is necessary to consider the mechanisms responsible for the photosensitizer accumulation in tumors. Photosensitizers administered directly into the bloodstream quickly reach and are

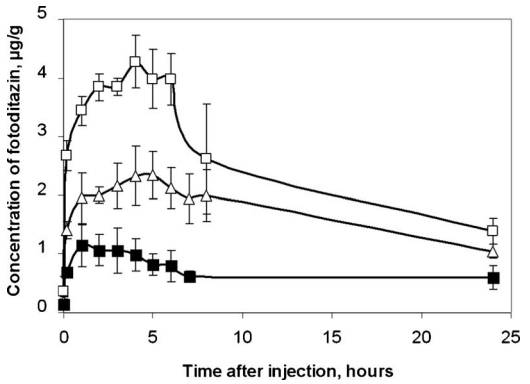

Fig. 5 Dose-dependent pharmacokinetics of fotoditazin (i.v.) in mouse cervical carcinoma *in vivo*; –□–, 25 mg/kg, –△–, 10 mg/kg, and –■–, 5 mg/kg. Each group included five mice. Error bars show standard deviation of the mean.

uptaken in the tumor. Thus, we observed intense fluorescence of photosens and fotoditazin in the tumor area at the early time instants after administration. The mechanisms involved in the preferential distribution of photosensitizers in tumors are not yet fully understood. This may be explained[50] by a number of factors, such as leaky vasculature, poorer lymphatic drainage, increased expression of low-density lipoprotein receptors on tumor cells and on tumor vascular endothelial cells, large fraction of macrophages, low extracellular pH. In the case with alasens, instead of a photosensitizer in synthetic form, its precursor is administered. Administration of 5-ALA induces biosynthesis of endogenous Pp IX *in situ* in tumors.[51] As a transformation of 5-ALA to Pp IX is a natural metabolic process including several enzymatic reactions, accumulation of Pp IX is relatively slow.

We compared the values of photosensitizer concentration in tissue *in vivo*, which we estimated by results of signal calibration in a model medium, with the data of other researchers obtained with tissue extraction methods.

We did not find information in the literature about the absolute concentrations of fotoditazin in tissues of small laboratory animals. Therefore, for comparison of the concentrations from fluorescence transillumination images with real values in tissues we will make use of a few works concerned with another fluorescent chlorin compound—mono-L-aspartyl chlorin e6. For the administered dose of 5 mg/kg, the photosensitizer concentration at maximum accumulation in tumor tissue (mice mammary carcinoma) amounted to 3.81 (Ref. 18) or 5.69 μg/g (Ref. 21). For a dose of 25 mg/kg, the concentration in the tumor grew[18] up to 14 μg/g.

The majority of papers concerned with studies of biodistribution and estimation of phthalocyanine photosensitizer concentrations in the organism of animals were carried out with high therapeutic doses.[19,52] In Ref. 19, it was specified that the phthalocyanine photosensitizer concentration in the tissue of radiation-induced fibrosarcoma of mice varied from 8.07 μg/g 4 h after injection to 21.95 μg/g 2 days after injection. The concentration of aluminium-chloride sulfated phthalocyanine obtained by Frisoli et al. for hamster cheek carcinoma was 5.6 μg/g 2 h after photosensitizer administration.[52] The concentration of Zn-naphthalocyanine in Lewis lung carcinoma tumor tissue 16 to 20 h after injection reached[53] 1.5 μg/g. Apparently, absolute values of phthalocyanine photosensitizer concentrations in tissues of experimental tumors are larger than those obtained by results of experiments in model media. This may be attributed to the difference in the used doses: the photosens dose (1 mg/kg) in our study was 10 times less than in the just mentioned works. For a Si-naphthalocyanine dose of 0.5 mg/kg, the photosensitizer concentration in tumor was commensurate with our assessed values. Twenty four hours after i.v. injection, the photosensitizer concentration in Lewis lung carcinoma tissue was 0.7 μg/g and in melanoma B16, 0.15 μg/g (Ref. 54).

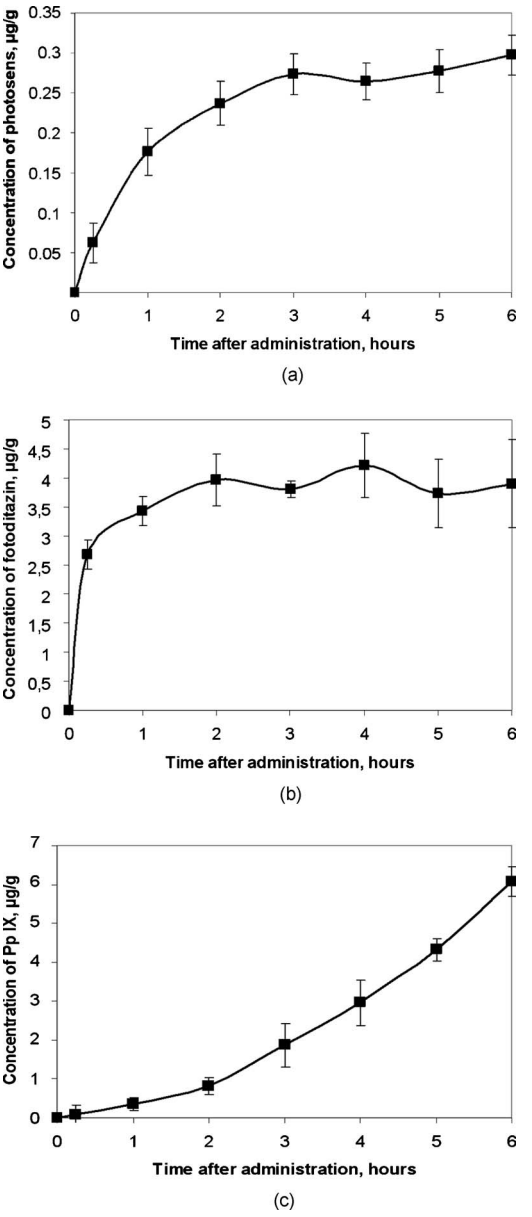

Fig. 6 Kinetics of *in vivo* tumor uptake of photosensitizers: (a) photosens (1 mg/kg), (b) fotoditazin (25 mg/kg), and (c) 5-ALA-induced Pp IX (alasens 400 mg/kg). Each group included five mice. Error bars show standard deviation of the mean.

According to the data on fluorescence transillumination imaging concentration of the 5-ALA-induced Pp IX in mouse cervical carcinoma 6 h after oral administration of the alasens

was about 6 μg/g. Our data are close to those of Perotti et al.[17] (5.23 μg/g), obtained with spectrofluorometery after tissue porphyrin extraction. Other authors reported lesser concentrations, for instance 2 μg/g (Ref. 20) and 1.54 μg/g (Ref. 55).

4 Conclusion

Current advances in fluorescence whole-body imaging and the chemistry of photosensitizers offer new opportunities for noninvasive *in vivo* assessment of drug pharmacokinetics in animal studies.[56] As was shown in Refs. 47 and 57–59, there is a great interest in direct measurements of the photosensitizer concentrations *in vivo*.

We demonstrated the possibility of *in vivo* investigation of photosensitizer pharmacokinetics by means of fluorescence transillumination imaging. Serial imaging in the same animal showed that this technique is able to estimate photosensitizer accumulation in transplantable tumor and washout over time (in individual animals). Quantification of the fluorescence in the tumor area provided an opportunity to define tumor uptake and retention kinetics.

For final conclusions on reliability of estimation of photosensitizer concentration by 2-D fluorescence images, elaborate experiments with use of standard tissue extraction methods are required. Even today, however, we can speak about the feasibility of measuring photosensitizer content in tumor with transillumination imaging technique.

Note that fotoditazin and alasens were used in therapeutic doses converted from humans to mice. Photosens was administered in a dose two times less than the therapeutic dose. Therefore, the sensitivity of the imaging setup is sufficient for effective visualization of fluorescent dyes in an animal study.

As transplantable tumors are indispensable for preclinical pharmacokinetics investigations of new photosensitizers, the demonstrated possibility of their visualization by transillumination imaging is extremely important in terms of a practical application of the technique.

Noninvasive assessment of pharmacokinetics by a transillumination imaging setup will allow rapid and cost-effective preclinical studies of newly developed photosensitizers for fluorescence diagnosis and PDT.

Acknowledgments

This work has been funded by the Russian Foundation for Basic Research (Project No. 09-02-97065) and the Science and Innovations Federal Russian Agency (projects 02.740.11.0086 and MD-3018.2009.7).

References

1. A. P. Castano, T. N. Demidova, and M. R. Hamblin, "Mechanisms in photodynamic therapy: part three—photosensitizer pharmacokinetics, biodistribution, tumor localization and modes of tumor destruction," *Photodiagn. Photodyn. Ther.* **2**(2), 91–106 (2005).
2. D. Wohrle, A. Hirth, T. Bogdahn-Rai, G. Schnurpfeil, and M. Shopova, "Photodynamic therapy of cancer: second and third generations of photosensitizers," *Russ. Chem. Bull.* **47**(5), 807–816 (1998).
3. H. van den Bergh and J.-P. Ballini, "Principles of photodynamic therapy," Chap. 2 in *Photodynamic Therapy of Ocular Diseases*, E. S. Gragoudas, J. W. Miller, and L. Zografos, Eds., pp. 11–42, Lippincott Williams & Wilkins, Philadelphia (2003).
4. D. Dolmans, D. Fukumura, and R. K. Jain, "Photodynamic therapy for cancer," *Nature Rev.* **3**, 380–387 (2003).
5. Z. Huang "A review of progress in clinical photodynamic therapy," *Technol. Cancer Res. Treat.* **4**(3), 283–293 (2005).
6. M. S. Thompson, A. Johansson, T. Johansson, S. Andersson-Engels, S. Svanberg, N. Bendsoe, and K. Svanberg "Clinical system for interstitial photodynamic therapy with combined on-line dosimetry measurements," *Appl. Opt.* **44**(19), 4023–4031 (2005).
7. H. Stepp, T. Beck, T. Pongratz, T. Meinel, F. W. Kreth, J. C. Tonn, and W. Stummer, "ALA and malignant glioma: fluorescence-guided resection and photodynamic treatment," *J. Environ. Pathol. Toxicol. Oncol.* **26**(2), 157–164 (2007).
8. K. A. Cengel, E. Glatstein, and S. M. Hahn, "Intraperitoneal photodynamic therapy," Part 6 in *Peritoneal Carcinomatosis*, W. P. Ceelen, Ed., pp. 493–514, Springer, New York (2007).
9. B. C. Wilson and M. S. Patterson, "The physics, biophysics and technology of photodynamic therapy," *Phys. Med. Biol.* **53**, R61–R109 (2008).
10. L. B. Josefsen and R. W. Boyle, "Photodynamic therapy and the development of metal-based photosensitisers," *Met. Based Drugs* **2008**, 276109 (2008).
11. K. Berg, P. K. Selbo, A. Weyergang, A. Dietze, L. Prasmickaite, A. Bonsted, B. Ø. Engesaeter, E. Angell-Petersen, T. Warloe, N. Frandsen, and A. Høgset, "Porphyrin-related photosensitizers for cancer imaging and therapeutic applications," *J. Microsc.* **218**(Pt. 2), 133–147 (2005).
12. L. R. Duska, M. R. Hamblin, J. L. Miller, and T. Hasan, "Combination photoimmunotherapy and cisplatin: effects on human ovarian cancer *ex vivo*," *J. Natl. Cancer Inst.* **91**(18), 1557–1563 (1999).
13. M. G. del Carmen, I. Rizvi, Y. Chang, A. C. E. Moor, E. Oliva, M. Sherwood, B. Pogue, and T. Hasan, "Synergism of epidermal growth factor receptor-targeted immunotherapy with photodynamic treatment of ovarian cancer *in vivo*," *J. Natl. Cancer Inst.* **97**(20), 1516–1524 (2005).
14. M. B. Vrouenraets, G. W. M. Visser, M. Stigter, H. Oppelaar, G. B. Snow, and G. A. M. S. van Dongen, "Targeting of aluminum (III) phthalocyanine tetrasulfonate by use of internalizing monoclonal antibodies: improved efficacy in photodynamic therapy," *Cancer Res.* **61**, 1970–1975 (2001).
15. P. McConville, W. L. Elliott, A. Kreger, R. Lister, J. B. Moody, E. Trachet, F. Urban, and W. R. Leopold, "Preclinical models of tumor growth and response," Chap. 2 in *In Vivo Imaging of Cancer Therapy*, A. F. Shields and P. Price, Eds., pp. 13–33, Humana Press Inc., Totowa, NJ (2007).
16. T. Corbett, L. Polin, P. LoRusso, F. Valeriote, C. Panchapor, S. Pugh, K. White, J. Knight, L. Demchik, J. Jones, L. Jones, and L. Lisow, "*In vivo* methods for screening and preclinical testing: Use of rodent solid tumors," Chap. 15 in *Anticancer Drug Development Guide: Preclinical Screening, Clinical Trials*, B. A. Teicher, P. A. Andrews, Eds., pp. 99–125, Humana Press Inc., Totowa, NJ (2004).
17. C. Perotti, A. Casas, H. Fukuda, P. Sacca, and A. Batlle, "ALA and ALA hexyl ester induction of porphyrins after their systemic administration to tumour bearing mice," *Br. J. Cancer* **87**, 790–795 (2002).
18. C. J. Gomer and A. Ferrario, "Tissue distribution and photosensitizing properties of mono-L-aspartyl chlorin e6 in a mouse tumor model," *Cancer Res.* **50**, 3985–3990 (1990).
19. J. Rousseau, R. Langlois, H. Ali, and J. E. Van Lier, "Biological activities of phthalocyanines XII: synthesis tumor uptake and biodistribution of 14C-labeled disulfonated and trisulfonated gallium phthalocyanine in C3H mice," *J. Photochem. Photobiol. B Biol.* **6**, 121–132 (1990).
20. G. D. Venosa, A. Batlle, H. Fukuda, A. MacRobert, and A. Casas, "Distribution of 5-aminolevulinic acid derivatives and induced porphyrin kinetics in mice tissues," *Cancer Chemother. Pharmacol.* **58**, 478–486 (2006).
21. A. Ferrario, D. Kessel, and C. J. Gomer, "Metabolic properties and photosensitizing responsiveness of mono-L-aspartyl chlorin e6 in a mouse tumor model," *Cancer Res.* **52**, 2890–2893 (1992).
22. S. Andrejevic Blant, T. M. Glanzmann, J.-P. Ballini, G. Wagnièrgres, H. van den Bergh, and P. Monnier, "Uptake and localisation of mTHPC (Foscan) and its 14C-labelled form in normal and tumour tissues of the hamster squamous cell carcinoma model: a comparative study," *Br. J. Cancer* **87**, 1470–1478 (2002).
23. R. Sroka, W. Beyer, L. Gossner, T. Sassy, S. Stocker, and R. Baumgartner, "Pharmacokinetics of 5-aminolevulinic-acid-induced porphyrins in tumour-bearing mice," *J. Photochem. Photobiol. B Biol.* **34**, 13–19 (1996).

24. N. I. Kazachkina, N. N. Zharkova, G. I. Fomina, R. I. Yakubovskaya, V. V. Sokolov, and E. A. Luk'yanets, "Pharmocokinetical study of Al- and Zn-sulphonated phthalocyanines," *Proc. SPIE* **2924**, 233–242 (1996).
25. M. R. Hamblin, M. Rajadhyaksha, T. Momma, N. S. Soukos, and T. Hasan, "*In vivo* fluorescence imaging of the transport of charged chlorin e6 conjugates in a rat orthotopic prostate tumour," *Br. J. Cancer* **81**(2), 261–268 (1999).
26. W. Zhong, J. P. Celli, I. Rizvi, Z. Mai, B. Q. Spring, S. H. Yun, and T. Hasan, "*In vivo* high-resolution fluorescence microendoscopy for ovarian cancer detection and treatment monitoring," *Br. J. Cancer* **101**, 2015–2022 (2009).
27. V. Ntziachristos, J. Ripoll, L. V. Wang, and R. Wesslender, "Looking and listening to light: the evolution of whole-body photonic imaging," *Nat. Biotechnol.* **23**, 313–320 (2005).
28. F. Leblond, S. C. Davis, P. A. Valdés, and B. W. Pogue "Pre-clinical whole-body fluorescence imaging: review of instruments, methods and applications," *J. Photochem. Photobiol. B Biol.* **98**(1), 77–94 (2010).
29. M. Hassan and B. A. Klaunber, "Biomedical applications of fluorescence imaging *in vivo*," *Compar. Med.* **54**(6), 635–644 (2004).
30. V. Ntziachristos, C. Bremer, and R. Weissleder, "Fluorescence imaging with near-infrared light: new technological advances that enable *in vivo* molecular imaging," *Eur. Radiol.* **13**, 195–208 (2003).
31. X. Montet, J.-L. Figueiredo, H. Alencar, V. Ntziachristos, U. Mahmood, and R. Weissleder, "Tomographic fluorescence imaging of tumor vascular volume in mice," *Radiology* **242**, 3 (2007).
32. U. Mahmood and R. Weissleder, "Near-infrared optical imaging of proteases in cancer," *Molecu. Cancer Ther.* **2**, 489–496 (2003).
33. J. V. Frangioni, "*In vivo* near-infrared fluorescence imaging," *Curr. Opin. Chem. Biol.* **7**, 626–634 (2003).
34. R. M. Hoffman, "Imaging in mice with fluorescent proteins: from macro to subcellular," *Sensors* **8**(2), 1157–1173 (2008).
35. M. Autiero, R. Cozzolino, P. Laccetti, M. Marotta, M. Quarto, P. Riccio, and G. Roberti, "Hematoporphyrin-mediated fluorescence reflectance imaging: application to early tumor detection *in vivo* in small animals," *Lasers Med. Sci.* **24**, 284–289 (2009).
36. V. Ntziachristos, G. Turner, J. Dunham, S. Windsor, A. Soubret, J. Ripoll, and H. A. Shih, "Planar fluorescence imaging using normalized data," *J. Biomed. Opt.* **10**, 064007 (2005).
37. B. W. Pogue, S. L. Gibbs, B. Chen, and M. Savellano, "Fluorescence imaging *in vivo*: raster scanned point-source imaging provides more accurate quantification than broad beam geometries," *Technol. Cancer Res. Treat.* **3**(1), 15–21 (2004).
38. C. Vinegoni, D. Razansky, S. A. Hilderbrand, F. Shao, V. Ntziachristos, and R. Weissleder, "Transillumination fluorescence imaging in mice using biocompatible upconverting nanoparticles," *Opt. Lett.* **34**(17), 2566–2568 (2009).
39. G. Zacharakis, H. Shih, J. Ripoll, R. Weissleder, and V. Ntziachristos, "Normalized transillumination of fluorescent proteins in small animals," *Mol. Imaging* **5**(3), 153–159 (2006).
40. J. Haller, D. Hyde, N. Deliolanis, R. de Kleine, M. Niedre, and V. Ntziachristos, "Visualization of pulmonary inflammation using noninvasive fluorescence molecular imaging," *J. Appl. Physiol.* **104**, 795–802 (2008).
41. I. V. Turchin, V. A. Kamensky, V. I. Plehanov, A. G. Orlova, M. S. Kleshnin, I. I. Fiks, M. V. Shirmanova, I. G. Meerovich, L. R. Arslanbaeva, V. V. Jerdeva, and A. P. Savitsky, "Fluorescence diffuse tomography for detection of red fluorescent protein expressed tumors in small animals," *J. Biomed. Opt.* **13**, 041310 (2008).
42. D. Kepshire, S. C. Davis, H. Dehghani, K. D. Paulsen, and B. W. Pogue, "Fluorescence tomography characterization for sub-surface imaging with protoporphyrin IX," *Opt. Express* **16**(12), 8581–8593 (2008).
43. E. A. Lukyanets, "Phthalocyanines as photosensitizers in the photodynamic therapy of cancer," *J. Porphyr. Phthalocyanines* **3**, 424–432 (1999).
44. L. A. Belyaeva, L. V. Adamyan, A. A. Stepanyan, K. G. Linkov, and V. B. Loshchenov, "Laser fluorescence spectroscopy with 5-aminolevulinic acid in operative gynecology," *Laser Phys.* **14**(9), 1207–1213 (2004).
45. A. V. Reshetnickov, G. V. Ponomarev, O. Y. Abakumova, T. A. Tsvetkova, A. V. Karmenyan, A. G. Rebeko, and R. P. Baum, "Novel drug form of chlorin e6," *Proc. SPIE* **3909**, 124–130 (2000).
46. Z. Hua, S. L. Gibson, T. H. Foster, and R. Hilf, "Effectiveness of δ-aminolevulinic acid-induced protoporphyrin as a photosensitizer for photodynamic therapy *in vivo*," *Cancer Res.* **55**, 1723–1731 (1995).
47. M. Harada, K. Aizawa, T. Okunaka, and H. Kato, "*In vivo* fluorescence kinetics of mono-L-aspartyl chlorin e6 (NPe6) and influence of angiogenesis in fibrosarcoma-bearing mice," *Int. J. Clin. Oncal.* **3**(4), 209–215 (1998).
48. V. A. Privalov, A. V. Lappa, O. V. Seliverstov, A. B. Faizrakhmanov, N. N. Yarovoy, E. V. Kochneva, M. V. Evnevich, A. S. Anikina, A. V. Reshetnicov, I. D. Zalevsky, and Y. V. Kemov, "Clinical trials of a new chlorin photosensitizer for photodynamic therapy of malignant tumors," *Proc. SPIE* **4612**, 178–189 (2002).
49. A. V. Ivanov, A. V. Reshetnickov, and G. V. Ponomarev, "One more PDT application of chlorin e6," *Proc. SPIE* **3909**, 131–137 (2000).
50. T. J. Dougherty, C. J. Gomer, B. W. Henderson, G. Jori, D. Kessel, M. Korbelik, J. Moan, and Q. Peng, "Photodynamic therapy," *J. Natl. Cancer Inst.* **90**(12), 889–905 (1998).
51. N. Fotinos, M. A. Campo, F. Popowycz, R. Gurny, and N. Lange, "5-Aminolevulinic acid derivatives in photomedicine: characteristics, application and perspectives," *Photochem. Photobiol.* **82**, 994–1015 (2006).
52. J. K. Frisoli, E. G. Tudor, T. J. Flotte, T. Hasan, T. F. Deutsch, and K. T. Schomacker, "Pharmacokinetics of a fluorescent drug using laser-induced fluorescence," *Cancer Res.* **53**, 5954–5961 (1993).
53. S. Müller, V. Mantareva, N. Stoichkova, H. Kliesch, A. Sobbi, D. Wöhrle, and M. Shopova, "Tetraamido-substituted 2, 3-naphthalocyanine zin (II) complexes as phototherapeutic agents: synthesis, comparative photochemical and photobiological studies," *J. Photochem. Photobiol. B. Biol.* **35**(3), 167–174 (1996).
54. V. Mantareva, M. Shopova, G. Spassov, D. Wöhrle, S. Muller, G. Jori, and F. Ricchelli, "Si (IV)-methoxyethylene-glycol-naphthalocyanine: synthesis and pharmacokinetic and photosensitizing properties in different tumour models," *J. Photochem. Photobiol. B. Biol.* **40**(3), 258–262 (1997).
55. R. G. Tunstall, A. A. Barnett, J. Schofield, J. Griffiths, D. I. Vernon, S. B. Brown, and D. J. H. Roberts, "Porphyrin accumulation induced by 5-aminolaevulinic acid esters in tumour cells growing *in vitro* and *in vivo*," *Br. J. Cancer* **87**, 246—250 (2002).
56. K. Licha and C. Olbrich, "Optical imaging in drug discovery and diagnostic applications," *Adv. Drug Delivery Rev.* **57**, 1087—1108 (2005).
57. C. C. Lee, B. W. Pouge, R. R. Strawbridge, K. L. Moodie, L. R. Bartholomew, G. C. Burke, and P. J. Hoopes, "Comparison of photosensitizer (AlPcS2) quantification techniques: in situ fluorescence microsampling versus tissue chemical extraction," *Photochem. Photobiol.* **74**(3), 453–460 (2001).
58. M. Canpolat and J. R. Mourant, "Monitoring photosensitizer concentration by use of a fiber-optic probe with a small source-detector separation," *Appl. Opt.* **39**(34), 6508–6514 (2000).
59. C. Sheng, B. W. Pogue, E. Wang, J. E. Hutchins, and P. J. Hoopes, "Assessment of photosensitizer dosimetry and tissue damage assay for photodynamic therapy in advanced-stage tumors," *Photochem. Photobiol.* **79**(6), 520–255 (2004).